

Development of CAD Model for MEMS Micropumps

M. Arik[§], S. M. Zurn[§], A. Bar-Cohen[§], Y. Nam[§], D. Markus[§], and D. Polla[§]

[§]Laboratory for Thermal Management of Electronics, Department of Mechanical Engineering,
University of Minnesota, Minneapolis, MN 55414

[§]Microtechnology Laboratory, Department of Electrical Engineering, University of Minnesota,
Minneapolis, MN 55414

ABSTRACT

This paper describes development of a Computer Aided Design Model for MicroElectroMechanical Systems. Finite Element Analyses have been completed successfully to understand the physical nature of the sample MEMS devices. Numerical results have been supported by analytical calculations in terms of the displacement, impedance, modular and harmonic analyses. A set of piezoelectrically actuated cantilever beams have been fabricated at the Microtechnology Laboratory of the University of Minnesota. Numerical results well compared with the experimental findings.

Keywords: CAD model, Finite element analyses, PZT cantilever beam, Atomic force microscope.

INTRODUCTION

Simulation is of vital importance in engineering applications and its power can be brought to bear on microfabricated devices. During the last days of the twentieth century, it is critical to obtain cheap, easy, and optimum solutions for practical engineering applications and research. Finite Element, Boundary Element, and Finite Volume methods can handle many problems impossible to solve with analytical techniques.

MEMS devices appear to have a promising future in many applications including those in the automobile industry, biological sciences, and many engineering disciplines [1]. Since MEMS are a new research area and there is a notable lack of material information related to thin films or applicable formulas, most of the fabrication has been done without any calculations, relying instead on the trial and error method. While this approach has led to many successful developments, it is highly inefficient, and can often cause wasting a large amount of money and time.

PZT cantilever beams and membranes are common in many MEMS applications such as microvalves, transducers, micropumps etc. Piezoelectric thin film cantilever beams (see Fig. 1) are designed and fabricated by applying surface micromachining techniques [2] and metal organic deposition of PZT [3]. In this study, the Finite Element Method is used to characterize the structural behavior of a

PZT cantilever beam. The thin film cantilever beams were formed using simple polycrystalline silicon phosphosilicate glass solid state surface micromachining techniques and metal-organic-precursor deposited on the membranes [3].

To obtain an optimum design Finite Element Analyses were performed for PZT thin film cantilever beams. Modular and harmonic analyses have been completed over the range of frequencies that the devices will be experiencing in the application. In the modal analyses, the first five important modes have been extracted and the natural frequencies are obtained.

Microfabrication of the Cantilever Beams

The devices were formed by using simple polycrystalline silicon-phosphosilicate glass solid state surface micromachining techniques [2] and an aqueous, metal-organic precursor for PZT [3]. Fig. 1 shows a schematic diagram of the cross sectional view of a PZT microcantilever. The beam is approximately 4.5 μm thick, 300 μm in width, and 1000 μm in length.

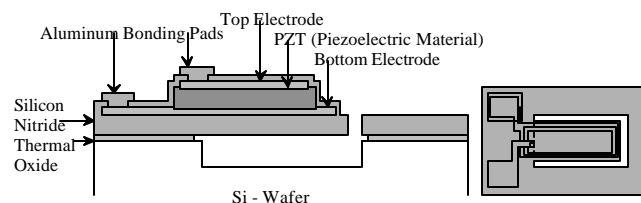


Figure 1: Cross section of a surface micromachined PZT microcantilever.

The first step is to dry etch a 1 μm well in the silicon wafer that allows the microcantilever to be planarized and be free from any unwanted stresses. The second step is to deposit and planarize a layer of thermal silicon dioxide and PSG for forming the spacer layer of the device. The next step is to deposit a layer of silicon nitride that will be used as the main material for the beams. Patterning and etching holes through the low stress nitride to the PSG layer is the fourth step. The PSG layer is then removed in HF vapor. The fifth step is to deposit a layer of low temperature silicon dioxide to seal the etch holes [4] and to avoid stiction problems. The sixth step is to deposit and pattern

the top and bottom electrodes, and PZT layer. The seventh step is to deposit and pattern a layer of PECVD silicon dioxide for electrical insulation of the electrodes when the bonding pads are deposited. The eighth step is to deposit and pattern a layer of aluminum to form the bonding pads. The final step is to pattern and dry etch through the PECVD silicon dioxide and silicon nitride to free the PZT microcantilever beam.

Fig. 2 shows the top view of the device taken by Scanning Electron Microscope at the end of the fabrication. A successful development of design and fabrication was completed and the five devices were chosen for the evaluation.

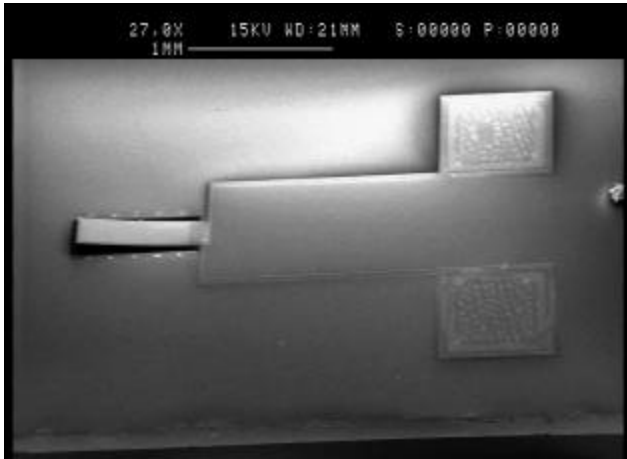


Figure 2: Schematic diagram of the PZT cantilever beam.

Experimental Results

Experimental study consisted of two different tests such as atomic force microscope and impedance analyzer tests. The first set of experiments was run on a Digital Instruments Dimension 3000 atomic force microscope (AFM). A function generator was used to actuate the microcantilever, and the photodetector of the AFM was used to measure the displacement of the tip of the microcantilever. The function generator was swept from 100 Hz to 2 MHz to determine the resonance points of the microcantilever. The resonance points of the microcantilever occurred at several frequencies such as 3, 24, 230, and 1400 kHz. Eq. 1 was used to determine how much power is need to displace the microcantilever beam at a given distance and a specified frequency.

$$\text{Power} = \frac{V^2}{|Z(\omega)|} \cos(\arg Z(\omega)) \quad (1)$$

where V is the voltage supplied by the function generator AFM, and $Z(\omega)$ is the impedance of the PZT capacitor.

Figs. 3 and 4 present the typical response of the beam from 0 to 80 kHz, and from 1415 to 1425 kHz respectively.

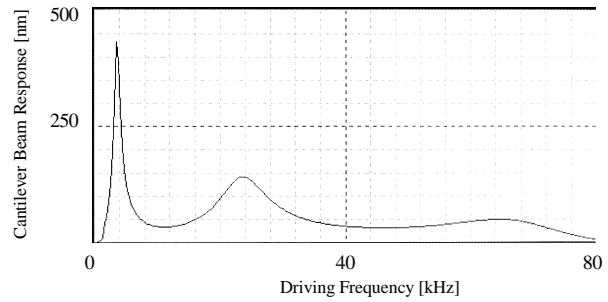


Figure 3: AFM results at low frequencies.

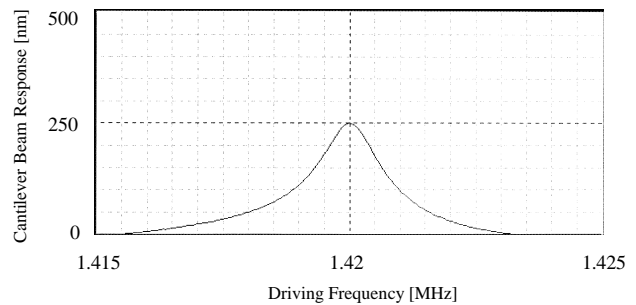


Figure 4: AFM results at high frequencies.

The next set of experiments was run on a HP 4194A Impedance phase analyzer. The output is a constant voltage and it measures the current necessary to maintain this constant voltage. As the impedance analyzer sweeps the frequency of the constant voltage source, the microcantilever beam will go through resonance at the same frequencies as seen on the AFM results. At each of the resonance frequencies the microcantilever beam will move much more than all other frequencies, and this motion will create a large stress in the PZT thin film. This stress will produce an excess charge on the electrodes, then this excess charge can be obtained experimentally by measuring the current flowing into the microcantilever. The impedance analyzer was swept from 100 Hz to 3 MHz to determine the major resonance points of the microcantilever. The major resonance points of the microcantilever which were observed, occurred at 230 kHz, 1.1 MHz, and 1.4 MHz. Fig. 5 shows a typical result from the impedance analyzer. Following the standard uncertainty analysis techniques [5], the measurements were found to be within $\pm 0.01\%$ in a range of $1\text{m}\Omega$ to $10\text{M}\Omega$, with a 95% confidence level.

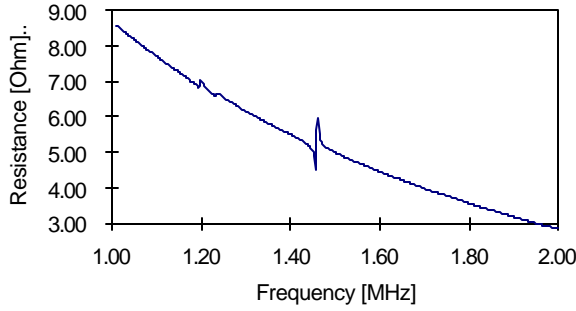


Figure 5: Impedance magnitude measurement.

Finite Element Analyses

Two kind of analyses, modal and harmonic, have been completed by employing ANSYS5.3 Finite Element software. To study the effect of meshing in modal and harmonic analyses, problem is solved for both fine and coarse mesh structures with a range of 100 to 15000 elements. However, there was no major difference in both solutions so the solutions were completed by applying a coarse mesh to save computer time. Zero displacement boundary conditions were applied in x, y and z directions at the root of the microcantilever beam and 600 elements were chosen for the meshing. With this meshing, it took about 1 minute per mode in the modal analyses and about 20 minutes in harmonic analyses for a range of 0 to 3 MHz on a SGI Onyx Reality 2 machine.

The first analysis was a modal analysis that is used to determine the vibration characteristics, such as natural frequencies and mode shapes of the cantilever beams. It was also a starting point for the harmonic analyses. The natural frequencies and mode shapes are important parameters in the design of a structure for dynamic loading conditions. The best way of determining the vibrational extracting modes is determining the specified frequency at which the devices will display range amplitudes of vibration.

The basic equation solved in a typical undamped modal analysis is the classical eigenvalue relation:

$$[K]\{\phi_i\} = \omega_i^2[M]\{\phi_i\} \quad (2)$$

Where $[K]$ is the stiffness matrix and $\{\phi_i\}$ is mode shape vector (eigenvector) of mode i , ω_i is the natural frequency of mode i (ω_i^2 is the eigenvalue), while $[M]$ is defined as mass matrix [6]. The Block Lanczos method was chosen to solve the eigenvalue problem as the most appropriate for these microbeams. This method applies the Lanczos recursion method. This is a highly accurate and fast method in comparison with other techniques. First five modes have been extracted with the specified frequency range of 0 and 3 MHz. Figs. 6 and 7 show typical results of the analysis for the first and second modes.

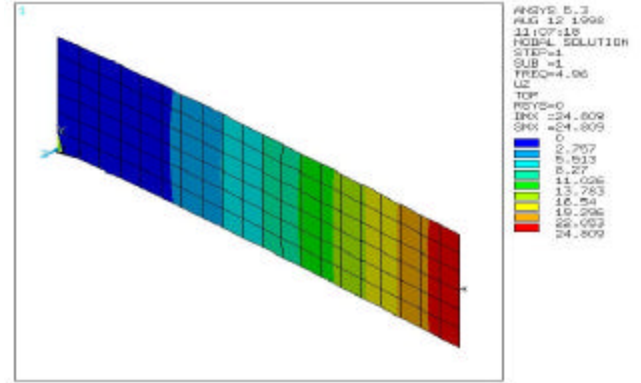


Figure 6: Frequency response of the beams at Mode 1.

The colored contours, with red a maximum and blue a minimum, show the deflections in the positive z-direction on the graphs. In Fig. 6, the maximum deflection is about 24.8 μm while the natural frequency is 4.96 kHz. The mode shape at the second mode shown in Fig. 7 is different than first mode. The natural frequency is obtained as 30.86 kHz while the maximum deflection was 24.8 μm .

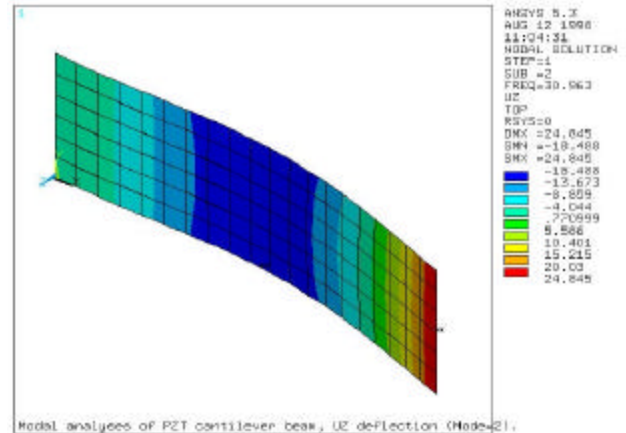


Figure 7: Frequency response of the beams at Mode 2.

A sustained cyclic load will produce a sustained cyclic response, a harmonic response, in a structural system. Harmonic response analysis can predict the sustained dynamic behavior of structures that will allow one to verify whether or not the design will successfully overcome resonance, fatigue, and other harmful effects of forced vibrations. Transient effects are assumed as negligible in the harmonic analyses. The applied force on the system can be represented as follows:

$$F = F_0 \cos(\omega t + \varphi) + F_0 \sin(\omega t + \varphi) \quad (3)$$

F_0 is amplitude of the applied force, while ωt is the phase angle. F_0 is calculated by using the analytical correlations and it is applied to the numerical model [6]. Fig. 8 shows

the results obtained from the FEM analysis and presents the maximum and the minimum deflections of the beam as a function of frequency.

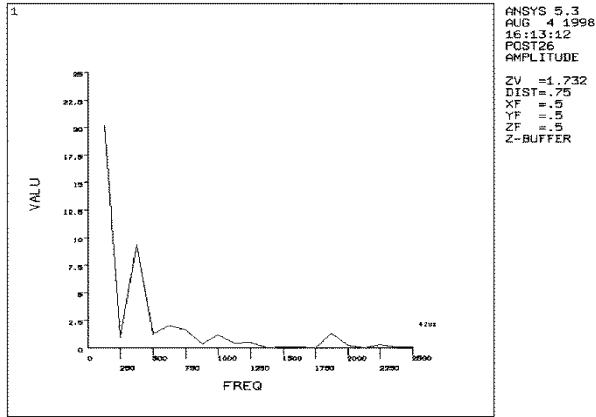


Figure 8: Resonance frequencies of the PZT beam from harmonic analyses.

ANSYS has the capability of applying the effects of temperature and pressure boundary conditions on the related elements of the structure, but this aspects will not be included in this paper.

RESULTS AND DISCUSSIONS

By examining the AFM results from Fig. 3, it is found that the first three resonant modes of the microcantilever occurred at 3.3, 24, and 64 kHz. Fig. 4 shows the next highest resonance frequency 1.42 MHz.

The ANSYS simulation provided results to be reached at a number of modes, although first two modes are presented here. Table 1 shows the results obtained from the impedance analyzer. It shows that the mean and standard deviation values at that experiments. It presents the mean frequencies and mean value of the resistance change on the devices. The last column presents the change of the resistance at the resonance frequency. \bar{x} is the mean value, σ is the standard deviation of the frequencies and resistance change in Table 1.

By comparing the frequency responses obtained in AFM and impedance analyzer experiments, it is observed that the two methods experimentally produce the same resonant frequencies within 1.27 % deviation. Fig. 8 shows the results obtained from harmonic analysis. A typical force (i.e. Eq. 3) is applied to the physical system and its response over a wide range of frequency is studied. When system reaches the resonance frequency, it has a peak displacement as seen on the Fig. 8. A similar behavior of the natural frequencies to the experimental findings was observed. However, as a result of the difficulty in obtaining

the exact force in z-direction on the piezoelectric layer, it is hard to obtain precise agreement.

Mode	\bar{x} [MHz]	σ [MHz]	\bar{x} [Ω]	σ [Ω]	\bar{x} %
1 st	0.23	0.0059	5.25	3.05	1.33
2 nd	1.17	0.035	1.21	0.64	1.86
3 rd	14.5	0.188	8.27	3.40	17.3

Table 1: Summary of the experimental HP 4194A magnitude resonant frequency results.

Future work will be aimed at experimentally determining the applied force with a small error that will allow one to compare better with the FEM findings.

SUMMARY AND CONCLUSIONS

The numerical analysis of microcantilever beams has been presented. A brief description of the fabrication process and experimental results are presented and they have been supported by numerical results. For the first three modes natural frequencies obtained from FEM analyses were very close to analytical results. After modal analyses has been completed, numerical solution of the devices are extended to the resonance frequencies by applying a harmonic driving force on the beams. The frequency range is chosen between 0 and 3 MHz and results showed similar behavior as experimental results obtained by using an atomic force microscope and impedance analyzer.

REFERENCES

- [1] S. A Campbell, "The Science and Engineering of Microelectronics Fabrication," Oxford University Press, 415-428, 1996.
- [2] R.T. Howe, J. Vac. Sci. Tech., B6, , pp. 1809 - 1813, 1988.
- [3] C.T. Lin, L. Li, J.S. Webb, M.S. Leung, and R.A. Lipeles, J. Electrochem. Soc., Vol. 142, No. 6, pp. 1957, June 1995.
- [4] S. Zurn, Q. Mei, C. Ye, T. Tamagawa, R. Collins, and D. L. Polla, IEEE International Electron Devices Meeting, Washington D. C., December 1991.
- [5] R. J. Moffat, "Describing the Uncertainties in Experimental Results", Experimental Thermal and Fluid Sciences, 3-17, 1988.
- [6] ANSYS 5.3, 1998.